Following Vegetative to Embryonic Cellular Changes in Leaves of Arabidopsis Overexpressing *LEAFY COTYLEDON2*[1][W][OPEN]

Mistianne Feeney[2], Lorenzo Frigerio, Yuhai Cui, and Rima Menassa*

Department of Biology, University of Western Ontario, London, Ontario, Canada N6A 5B7 (M.F., Y.C., R.M.); Southern Crop Protection and Food Research Centre, Agriculture and Agri-Food Canada, London, Ontario, Canada N5V 4T3 (M.F., Y.C., R.M.); and School of Life Sciences, University of Warwick, Coventry CV4 7AL, United Kingdom (L.F.)

ORCID ID: 0000-0003-3536-0332 (R.M.).

Embryogenesis in flowering plants is controlled by a complex interplay of genetic, biochemical, and physiological regulators. LEAFY COTYLEDON2 (LEC2) is among a small number of key transcriptional regulators that are known to play important roles in controlling major events during the maturation stage of embryogenesis, notably, the synthesis and accumulation of storage reserves. *LEC2* overexpression causes vegetative tissues to change their developmental fate to an embryonic state; however, little information exists about the cellular changes that take place. We show that LEC2 alters leaf morphology and anatomy and causes embryogenic structures to form subcellularly in leaves of Arabidopsis (*Arabidopsis thaliana*). Chloroplasts accumulate more starch, the cytoplasm fills with oil bodies, and lytic vacuoles (LVs) appear smaller in size and accumulate protein deposits. Because LEC2 is responsible for activating the synthesis of seed storage proteins (SSPs) during seed development, SSP accumulation was investigated in leaves. The major Arabidopsis SSP families were shown to accumulate within small leaf vacuoles. By exploiting the developmental and tissue-specific localization of two tonoplast intrinsic protein isoforms, the small leaf vacuoles were identified as protein storage vacuoles (PSVs). Confocal analyses of leaf vacuoles expressing fluorescently labeled tonoplast intrinsic protein isoforms reveal an altered tonoplast morphology resembling an amalgamation of a LV and PSV. Results suggest that as the LV transitions to a PSV, the tonoplast remodels before the large vacuole lumen is replaced by smaller PSVs. Finally, using vegetative and seed markers to monitor the transition, we show that LEC2 induces a reprogramming of leaf development.

The transition between seed and vegetative development involves considerable changes in cellular processes. Two major cellular events that demarcate seed and vegetative growth are the accumulation and catabolism of storage reserves. Arabidopsis (*Arabidopsis thaliana*) seeds accumulate high levels of lipids and proteins and a comparatively lower level of carbohydrate reserves in the form of starch. These reserves are stored in specialized seed organelles. In Arabidopsis, seed storage proteins (SSPs) are accumulated in protein storage vacuoles (PSVs), while triacylglycerols (TAGs) are stored in oil bodies and starch is found in plastids (Mansfield and Briarty, 1992; Baud et al., 2008). Upon germination, these reserves serve as a nutrient source to sustain the growing seedling until it becomes photoautotrophic (Penfield et al., 2006).

In seed plants, embryogenesis is divided into two phases. During the morphogenesis phase, the embryo takes shape, and during the maturation phase, reserves are synthesized to prepare the embryo for developmental arrest and for subsequent germination (Harada, 2001). During the evolution of seeds, the maturation phase was integrated into the life cycle of flowering plants (Vicente-Carbajosa and Carbonero, 2005). For this to happen, regulatory programs that control the maturation phase have evolved within the seed development program (Zhang and Ogas, 2009; Willmann et al., 2011). Through the analysis of mutants impaired in seed formation and by overexpression of individual seed genes in vegetative tissues, key positive transcriptional regulators of the maturation phase, *LEAFY COTYLEDON1* (*LEC1*; West et al., 1994), *LEC2* (Stone et al., 2001), *FUSCA3* (*FUS3*; Bäumlein et al., 1994; Keith et al., 1994), and *ABSCISIC ACID INSENSITIVE3* (*ABI3*; Giraudat et al., 1992; Parcy et al., 1994; Nambara et al., 1995), were identified. These regulators act in a partially redundant manner to initiate and control seed maturation and to prevent germination. They achieve this control through interactions within a complex seed regulatory network (Santos-Mendoza et al., 2008).

[1] This work was supported by the A-Base Funding Program of Agriculture and Agri-Food Canada and the Leverhulme Trust (grant no. RPG–327).

[2] Present address: School of Life Sciences, University of Warwick, Coventry CV4 7AL, United Kingdom.

* Corresponding author; e-mail rima.menassa@agr.gc.ca.

The author responsible for distribution of materials integral to the findings presented in this article in accordance with the policy described in the Instructions for Authors (www.plantphysiol.org) is: Rima Menassa (rima.menassa@agr.gc.ca).

[W] The online version of this article contains Web-only data.

[OPEN] Articles can be viewed online without a subscription.

www.plantphysiol.org/cgi/doi/10.1104/pp.113.220996

Ectopic expression of *LEC2* revealed its ability to confer embryogenic characteristics in vegetative tissues and even to induce the formation of somatic embryos (Stone et al., 2001). *LEC2* activity up-regulates the expression of *oleosin*, *SSP*s, *LEC1*, *FUS3*, and *ABI3* RNAs (Kroj et al., 2003; Santos-Mendoza et al., 2005; Braybrook et al., 2006; To et al., 2006) and is involved in controlling plant growth regulator activity (Braybrook et al., 2006; Stone et al., 2008) and in regulating soluble sugar and starch pathways (Angeles-Núñez and Tiessen, 2011). A number of *LEC2* activities associated with seed gene promoter targets and interactions within the seed regulatory network have been elucidated (Braybrook et al., 2006; Santos-Mendoza et al., 2008). However, our knowledge of the events that occur at the cellular level is limited. Given that LEC2 exerts control over the cellular environment to promote the metabolic changes involved in embryo development (Petrie et al., 2010), we were interested in studying the detailed cellular changes that take place as *LEC2* is overexpressed in Arabidopsis leaves. Here, we show that *LEC2* overexpression confers embryogenic characteristics to leaves. The morphology of leaves begins to resemble cotyledons. At the cellular level, the leaf anatomy is modified and is characterized by the formation of embryogenic structures. We were interested in the fate of vacuoles, which are prominent organelles present during both vegetative and seed development. We found that *LEC2* overexpression caused leaf lytic vacuoles (LVs) to transition to PSVs. Using vegetative and seed markers to monitor the vegetative-to-embryonic transition, we show that LEC2 induces a reprogramming of leaf development.

RESULTS

LEC2 Overexpression Alters Leaf Morphology to Resemble Cotyledons

Previous studies have overexpressed *LEC2* to elucidate its regulatory activities and have elegantly demonstrated its central role in coordinating embryo development (Stone et al., 2001, 2008; Santos-Mendoza et al., 2005; Braybrook et al., 2006). However, little focus was paid to the alterations that arise in vegetative cells by *LEC2* overexpression. Thus, we investigated these effects in Arabidopsis leaves. A *35S:LEC2-GR* Arabidopsis overexpression line was used in this study (Stone et al., 2008). The steroid-binding domain of the glucocorticoid receptor (GR) acts as a selective inducer of LEC2 function, thereby allowing the flexibility to activate LEC2 when desired by incubating plants with a synthetic steroid, dexamethasone (DEX; Sablowski and Meyerowitz, 1998).

LEC2 overexpression promoted a change in leaf phenotype from vegetative to embryogenic characteristics. While ecotype Wassilewskija (Ws-0) plants were not affected by either dimethyl sulfoxide (DMSO) or DEX (Fig. 1, A–C) and *LEC2* plants were not affected by DMSO (Fig. 1, D and E), plants overexpressing *LEC2* were easily distinguished from controls by 14 d on DEX (Fig. 1, F and H). These plants were much smaller than controls and had smaller, curled leaves and shorter petioles. Leaves resembled cotyledons; they were fleshy with smooth, round leaf margins and a reduced number of trichomes (Fig. 1, G and H).

LEC2 Overexpression Promotes an Embryonic Leaf Anatomy and Composition

To establish whether changes in leaf morphology are associated with changes in leaf anatomy, leaf sections were stained with toluidine blue-O (TBO). TBO binds to most cellular components except starch and lipids (Regan and Moffatt, 1990) and is commonly used to identify PSVs (Shimada et al., 2003). A survey of leaves from all treatments shown in Figure 1 revealed that the leaf anatomy of all control treatments was similar (Supplemental Fig. S1, A–E). In these leaf sections, the

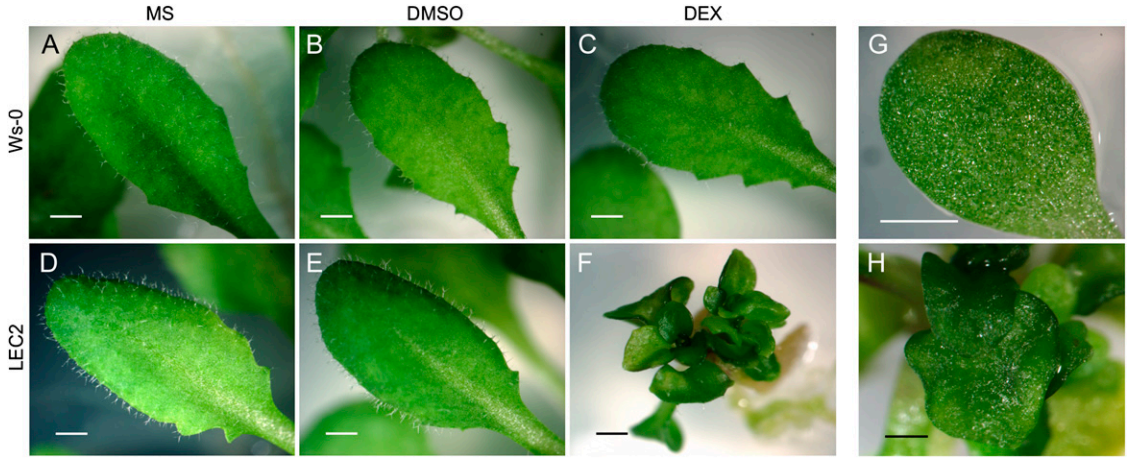

Figure 1. *LEC2* overexpression alters the leaf morphology to resemble cotyledon-like organs. A to C, Ws-0 plants incubated on MS medium (A) or MS supplemented with DMSO (B) or 30 μM DEX (C). D to F, *LEC2* plants incubated on MS medium (D), or MS supplemented with DMSO (E) or 30 μM DEX (F). G and H, Ws-0 cotyledon from 7-d-old seedling on MS medium (G) is compared with a leaf from a *LEC2* plant treated with 30 μM DEX (H). Bars = 1 mm (A–E and G) and 0.8 mm (F and H).

palisade and spongy mesophyll layers can usually be distinguished by their shape. Given that the appearance of control leaf treatments were alike, only representative leaf control treatments are shown in subsequent work.

The leaf anatomy was remarkably altered in leaves overexpressing *LEC2*. In contrast to control plants (Fig. 2A), leaf mesophyll layers were no longer distinguishable in induced *LEC2* plants (Supplemental Fig. S1F; Fig. 2B). Cells were arranged much closer together, their shape was altered, and intracellular spaces were densely stained. Vacuoles were drastically reduced in size, and the vacuolar lumen was lightly stained by TBO (Fig. 2B). The anatomy of induced *LEC2* leaves resembled that of seed tissues in the organization and shape of cells. However, within seed cells, heavily stained PSVs are surrounded by unstained lipid reserves (Fig. 2C).

To identify the composition of leaf cells overexpressing *LEC2*, three histochemical stains were chosen, each specific for different cell components. Under our experimental conditions, TBO stains proteins blue, osmium tetroxide (OsO_4) stains lipids black, and iodide potassium iodine (IKI) binds to starch and produces a red color. Control leaf cells contained large unstained LVs, which occupied most of the cell space, while the cytoplasm,

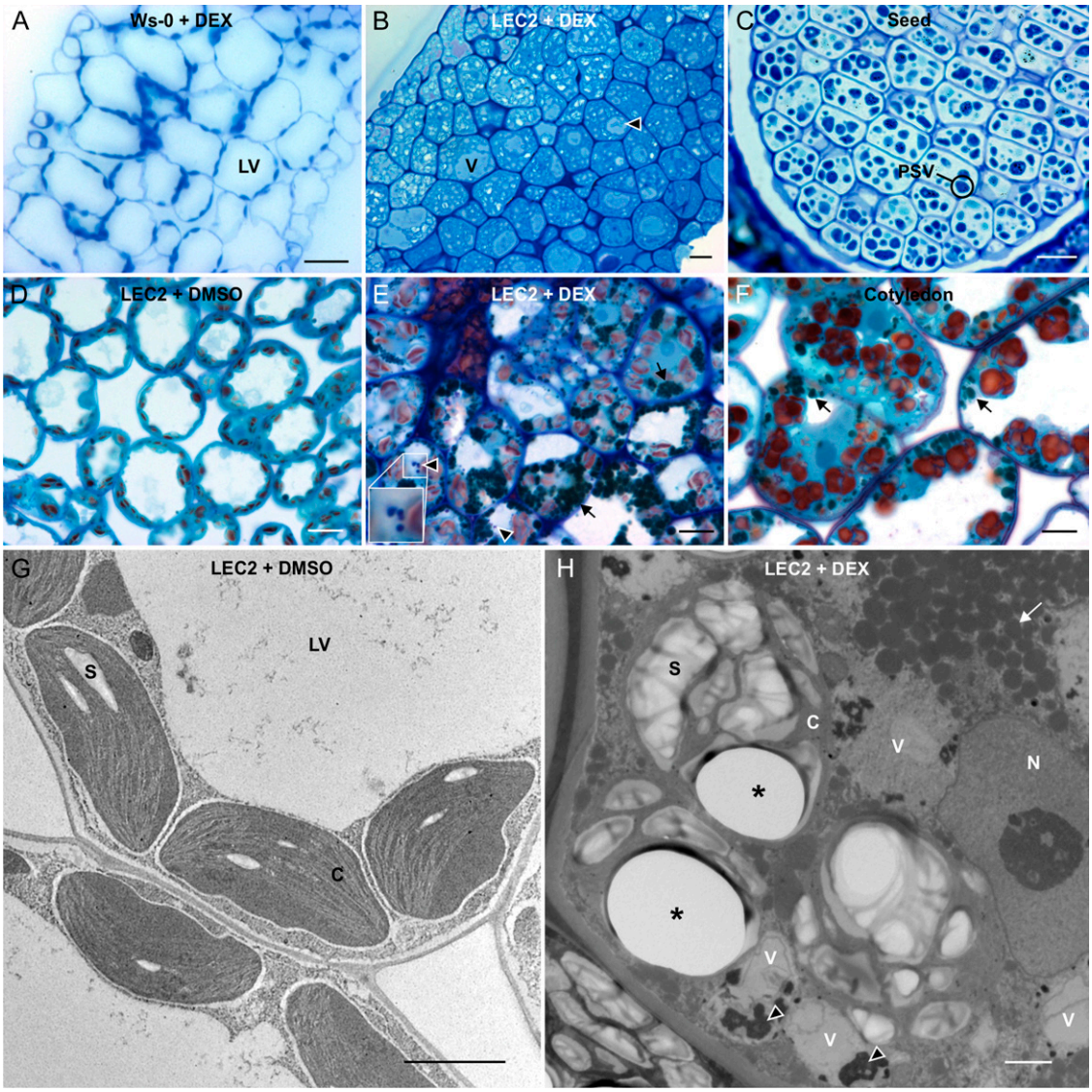

Figure 2. *LEC2* overexpression promotes embryonic leaf anatomy and composition. A to C, Leaf sections from Ws-0 plants exposed to DEX (A), *LEC2* plants exposed to DEX (B), or Ws-0 seed sections (C) were stained with TBO and imaged by light microscopy. D to F, Leaf sections from *LEC2* plants exposed to DMSO (D) or DEX (E) or cotyledons from 7-d-old *LEC2* seedlings (F) were stained with TBO (blue), IKI (red), and OsO_4 (black) and imaged by light microscopy. G and H, *LEC2* plants exposed to DMSO (G) or DEX (H) were stained with OsO_4 and imaged by transmission electron microscopy. Arrowheads point to protein aggregates and arrows point to lipid-filled vesicles. C, Chloroplast; LV, lytic vacuole; N, nucleus; PSV, protein storage vacuole (circled); S, starch granule; V, vacuole. Asterisks indicate sectioning artifacts. Bars = 20 μm (A and B), 15 μm (C), 10 μm (D–F), and 2 μm (G and H).

other organelles, and the cell membrane and wall were stained blue, and red starch granules were observed inside chloroplasts (Fig. 2D). In cotyledons from 7-d-old seedlings, LVs appeared smaller in size, a higher volume of cytoplasm was present, and starch granules were much larger than in leaf cells (Fig. 2F). In addition, black-stained, lipid-filled organelles were observed in the cytoplasm of cotyledon cells. These are most likely oil bodies that were accumulated during seed maturation (Mansfield and Briarty, 1996). Triple staining of induced *LEC2* leaf sections revealed an appearance more similar to cotyledon than leaf tissue (Fig. 2E). Compared with control leaves, induced *LEC2* leaf cells had an increased volume of cytoplasm that contained abundant lipid-filled structures. Vacuoles were reduced in size and starch granules were enlarged. Furthermore, TBO-stained deposits were present within the small vacuoles, suggesting that they contain protein (Fig. 2E, inset).

Transmission electron microscopy revealed similar observations. In contrast to control leaf cells (Fig. 2G), induced *LEC2* leaf cells possessed a higher volume of cytoplasm containing novel osmium-stained globular structures, similar to the lipid-filled structures observed in triple-stained sections (Fig. 2, E and H). The LV was reduced in size and appeared to be fragmented into smaller vacuoles containing electron-opaque aggregates, which correlate with the TBO-stained deposits observed in triple-stained tissues (Fig. 2, E and H). These aggregates may represent protein deposits. We also observed numerous holes in the resin-embedded tissue upon sectioning of the induced *LEC2* tissues (Fig. 2H). The holes were all associated with enlarged starch granules present in chloroplasts of induced *LEC2* leaves but did not occur in leaf samples from control treatments. Our results show that induced *LEC2* leaf cells accumulate lipids, starch, and protein deposits.

Oil Bodies Accumulate in the Cytoplasm of Induced *LEC2* Leaf Cells

To characterize the lipid-filled structures observed upon induction of LEC2 (Fig. 3A), we investigated if they could be oil bodies, organelles commonly found in seed and cotyledons (Kim et al., 2002). For this, immunogold electron microscopy was carried out using an antibody against oleosin, a transmembrane protein that serves to control the size, shape, and stability of oil bodies (Siloto et al., 2006; Shimada et al., 2008). No specific labeling was observed in leaves derived from *LEC2* plants incubated with DMSO (Fig. 3B). However, in induced *LEC2* leaf cells, the antibody labeled the edge of the novel structures (Fig. 3C) with the same sparse labeling pattern as observed in seeds (Fig. 3D), indicating that the structures are oil bodies. Their accumulation in leaves demonstrates the ability of LEC2 to promote the formation of these seed-specific organelles in vegetative tissues.

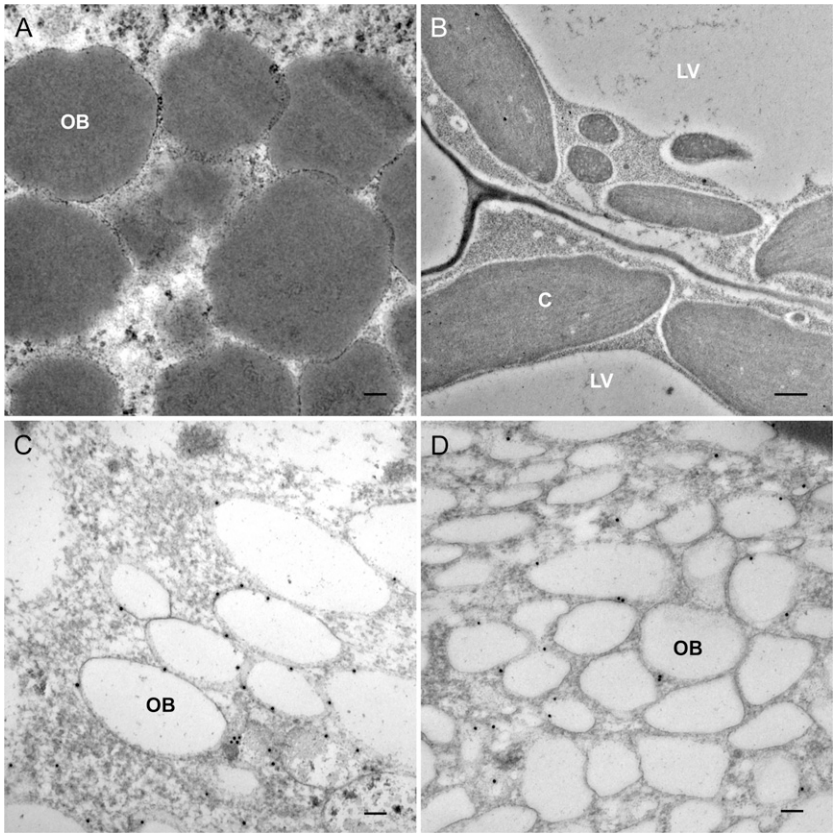

Figure 3. LEC2 promotes the accumulation of oil bodies in leaf cells. Oil bodies stained with OsO_4 in a leaf section from *LEC2* plants incubated with DEX (A). Immunolabeling of oleosin in leaf sections from *LEC2* plants incubated on DMSO (B) or DEX (C) or Ws-0 seed sections (D). C, Chloroplast; LV, lytic vacuole; OB, oil body. Bars = 100 nm (A, C, and D) and 500 nm (B).

Chloroplasts Accumulate Large Starch Granules in Response to LEC2 Overexpression

Because DEX-induced *LEC2* leaves display an increase in the size and number of starch granules when compared with control leaves (Fig. 2), we undertook a more detailed microscopic and quantitative analysis of starch deposition and accumulation in these leaves. Chloroplasts of uninduced *LEC2* plants displayed the typical phenotype of wild-type chloroplasts, with few, if any, starch grains (Fig. 4A). However, in induced *LEC2* leaves, the starch granules increase in number and in size. In addition, localized areas were packed with small cells containing dense deposits of starch granules (Fig. 4B). In many instances, the chloroplasts were so tightly filled with starch granules that it was often difficult to discern the inner chloroplast structure. To correlate the observed phenotype with starch accumulation levels, quantitative data for leaf starch content were collected from induced and control plants (Fig. 4C). Results showed that induced *LEC2* leaves store over 6-fold more starch reserves compared with control leaves.

SSPs Accumulate in Induced *LEC2* Leaves and Are Localized to Small Vacuoles

Given that putative protein deposits were detected in small-sized vacuoles of induced *LEC2* leaves using light and electron microscopy (Fig. 2, E and H) and that *SSP* RNA is present in Arabidopsis leaves overexpressing *LEC2* (Santos-Mendoza et al., 2005; Braybrook et al., 2006), the accumulation of SSPs was examined in these leaves. Seed proteins were detected with antibodies against the two major Arabidopsis SSP families (Kroj et al., 2003; Baud et al., 2008), the 12S globulins (Shimada et al., 2003) and 2S albumins (Scarafoni et al., 2001). Both antibodies detected SSPs from seed extracts and induced *LEC2* leaves but not from control leaves (Fig. 5A). Thus overexpression of *LEC2* caused SSPs to accumulate in leaves where they do not normally occur (Gruis et al., 2004).

SSPs usually accumulate in PSVs in Arabidopsis seeds (Mansfield and Briarty, 1992). In induced *LEC2* leaf cells, immunogold electron microscopy showed that both 2S and 12S SSPs accumulate in electron-opaque aggregates (Fig. 5, C and D) present within small vacuoles. These protein deposits were often observed accumulating in clumps along the luminal side of the tonoplast or aggregated within the vacuolar lumen (Fig. 5B). To demonstrate that 2S and 12S antibodies were effective in immunolocalizing SSPs, seed sections were used as positive controls. For both antibodies, gold particles localized to the PSV matrix (Fig. 5, E and F).

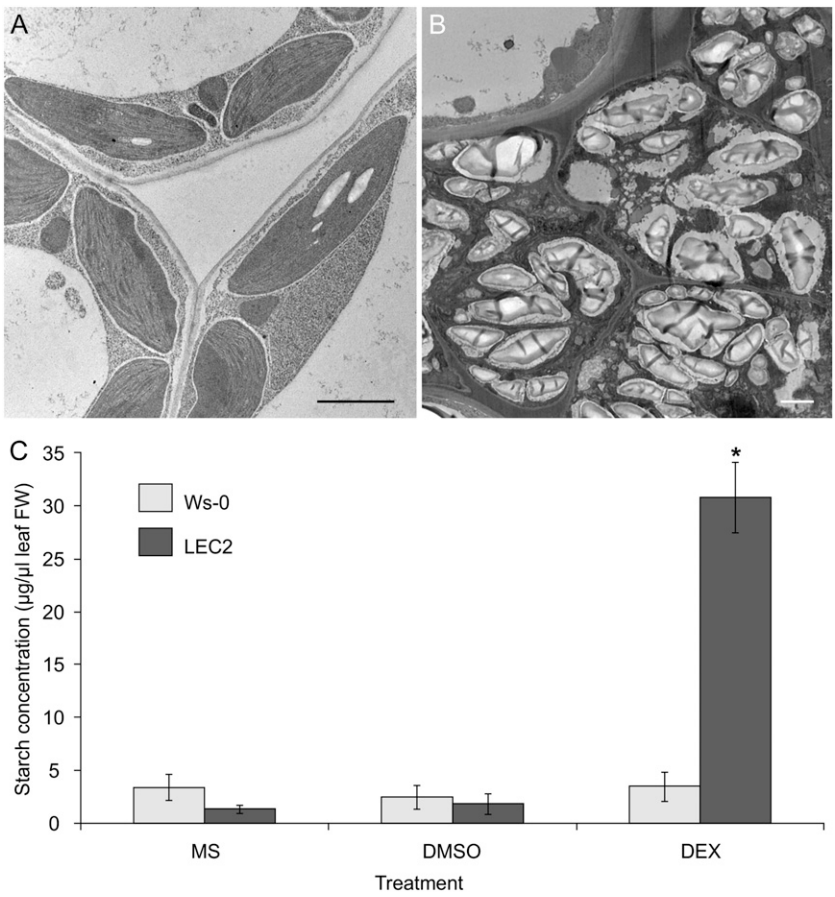

Figure 4. *LEC2* overexpression promotes increased starch accumulation in leaves. A and B, Small starch granules were observed in leaf chloroplasts of *LEC2* plants on DMSO (A). Starch granules increased in size and number, and dense starch deposits were observed in discrete areas of induced *LEC2* leaf sections (B). Bars = 2 μm. C, Starch accumulation in leaves after 14 d on treatments. Ws-0 or *LEC2* plants were incubated on MS medium alone or supplemented with DMSO or DEX. Standard errors are indicated. Asterisk indicates significant difference from control (Student's *t* test, $P < 0.01$).

Small-Sized Vacuoles Appearing in Induced *LEC2* Leaves Are PSVs

In *LEC2* plants induced by DEX, SSPs accumulate in electron-opaque aggregates within organelles that resemble small vacuoles. To confirm that these organelles are vacuoles and to further characterize them, tonoplast intrinsic proteins (TIPs) were used as markers. TIPs are members of a subfamily of transmembrane proteins called aquaporins, which form channels to transport water and small molecules across the tonoplast (Maurel et al., 2009). Arabidopsis has 10 TIP isoforms, and their expression patterns are developmentally and spatially controlled. In Arabidopsis, *TIP3;1* (*α-TIP*) is highly expressed on the tonoplast of PSVs in embryos during seed development. As the seed germinates, *TIP3;1* expression declines and is replaced by *TIP1;1* (*γ-TIP*) expression. TIP1;1 localizes to the tonoplast of LVs and is the most widely expressed TIP in vegetative tissues (Jauh et al., 1999; Johanson et al., 2001; Hunter et al., 2007; Beebo et al., 2009; Gattolin et al., 2009, 2010, 2011). Therefore the pattern of endogenous *TIP3;1* expression was exploited to determine whether the small leaf vacuoles observed in leaves overexpressing *LEC2* could be storage vacuoles.

Incubation of induced *LEC2* leaf tissue with an antibody raised against TIP3;1 (Jauh et al., 1998) showed specific labeling along the tonoplast of the small vacuoles where the electron-opaque aggregates are present (Fig. 6A). The TIP3;1 antibody did not label the LV tonoplast in control, uninduced leaf tissue (Fig. 6B) but localized to the PSV tonoplast in seed tissue (Fig. 6C), demonstrating its specificity for the TIP3;1 protein. These results suggest that in leaves overexpressing *LEC2*, small vacuoles containing electron-opaque SSP

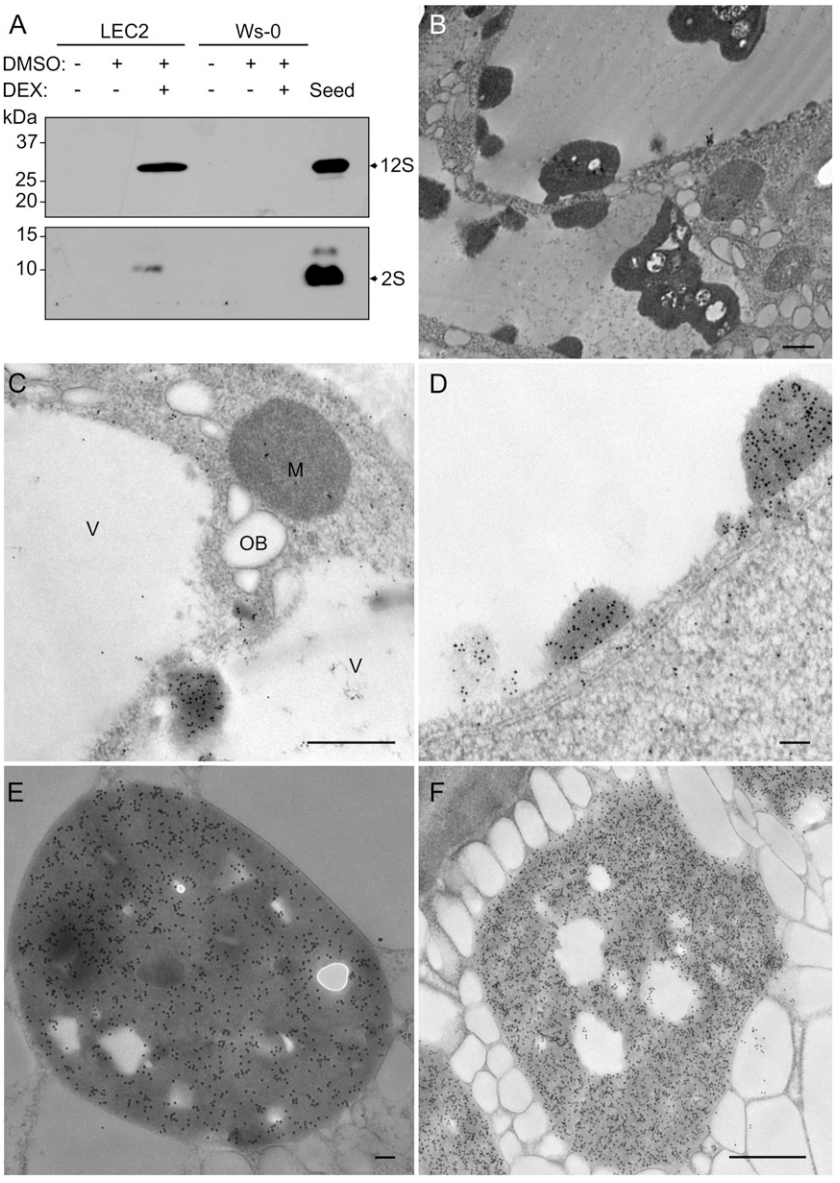

Figure 5. SSPs accumulate in induced *LEC2* leaves and are localized to aggregates within small vacuoles. A, Antibodies against 12S globulins and 2S albumins were used to detect proteins by immunoblots. Arrows point to seed protein bands. B, A low-magnification image of aggregates accumulating in small vacuoles forming in induced *LEC2* leaf cells. C and D, Immunolocalization of SSPs in leaves of *LEC2* plants exposed to DEX for 14 d. Antibodies localized 12S (C) and 2S (D) proteins to electron-opaque aggregates within the lumen of small leaf vacuoles. E and F, Immunolocalization of SSPs in Ws-0 seed tissue. 12S (E) and 2S (F) proteins were localized to the PSV matrix. Ten-nanometer gold particles were used (C–F). M, Mitochondrion; OB, oil body; V, vacuole. Bars = 500 nm (B, C, and F) and 100 nm (D and E).

aggregates represent a transitional stage from a LV to a PSV.

An Examination of the Transition of Leaves from a Vegetative to an Embryonic State

Our results have so far illustrated a snapshot of the leaf cell biology of plants overexpressing *LEC2* at 14 d on DEX. To provide a more thorough view of the alterations to induced *LEC2* leaf cells over time, samples were collected every 3 to 4 d over a 21-d period to examine the pattern of protein accumulation and the alteration of cell fate.

To monitor the progression of the transition from vegetative to embryonic characteristics caused by *LEC2* overexpression, the accumulation pattern of vegetative (TIP1;1) and seed-specific (TIP3;1, 12S globulin, and oleosin) protein markers was followed in leaves over time. Protein was extracted from leaves and analyzed by immunoblot. Representative blots are shown in Figure 7. Leaves collected from control uninduced *LEC2* plants (–DEX) did not accumulate seed proteins over the 21-d period but did present accumulation of TIP1;1. However, in induced *LEC2* plants (+DEX), seed proteins were first detected in leaves at 11 d and in all subsequent leaf samples for the duration of the experiment. Conversely, the TIP1;1 vegetative protein marker disappeared from induced *LEC2* leaf samples after 11 d on DEX. Smaller bands were observed on the oleosin, TIP1;1, and TIP3;1 blots, which may be due to proteolytic cleavage of the transmembrane domains of these proteins (Jauh et al., 1999; Hope et al., 2002). Degradation of TIP3 isoforms can also be observed by confocal microscopy. In embryos coexpressing *TIP3;1-yellow fluorescent protein* (*YFP*) and *TIP3;2-mCherry* (Supplemental Fig. S2, A–C), both proteins label the PSV tonoplast quite clearly (Gattolin et al., 2011). However, substantial TIP3;2-mCherry fluorescence is observed in the PSV lumen, which reveals degradation of the TIP fusion. The enhanced stability of red fluorescent protein (RFP) and its variants (such as mCherry) over GFP and its variants (such as YFP) within the acidic vacuole lumen is thought to account for the discrepancy between the two fluorescent proteins (Tamura et al., 2003; Shaner et al., 2005). Thus, degradation of TIP isoforms in induced *LEC2* tissues is to be expected. Nevertheless, TIP3;1-YFP still labels the tonoplast quite clearly at this stage (Supplemental Fig. S2, D–F).

To follow the alteration of cell fate in leaves overexpressing *LEC2*, we stained leaf sections collected over time. *LEC2* leaf sections treated with DMSO looked similar among all collection days (Supplemental Fig. S3, A–F). By contrast, *LEC2* leaf sections induced by DEX revealed phenotypic changes that became more pronounced over time. Already at 4 and 7 d of incubation on DEX, chloroplasts had large starch granules, small oil bodies were visible in the cytoplasm, and vacuoles were slightly reduced in size (Supplemental Fig. S3, G and H). By 11 to 14 d of incubation on DEX, the space between cells was reduced, vacuoles were extremely reduced in size, oil bodies were more plentiful and larger in size, and small protein deposits were observed in the small vacuoles (Supplemental Fig. S3, I and J). As more time was spent on DEX, the staining intensity of starch and lipid reserves became more pronounced, and, consequently, specimens were more difficult to visualize using light microscopy (Supplemental Fig. S3, K and L). In summary, alteration of the leaf cell fate toward embryogenic characteristics was seen as early as 4 d after incubation on DEX, was obvious by 11 d on DEX, and became more prominent over time on DEX. Taken together, the alteration of leaf cell fate illustrated by light microscopy (Supplemental Fig. S3) correlates well with seed protein accumulation patterns in response to *LEC2* overexpression (Fig. 7).

LV to PSV Transition in Leaves following LEC2 Induction

To study the LV to PSV transition in vegetative tissues of induced *LEC2* plants, the expression pattern of

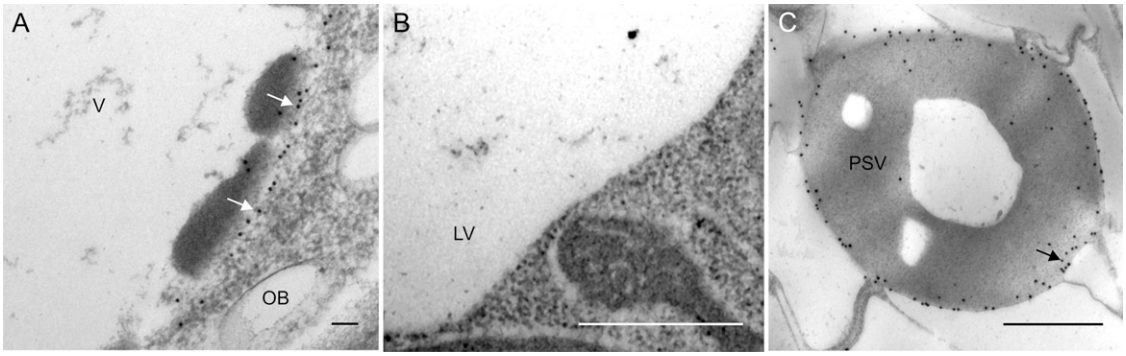

Figure 6. Small vacuoles arising in leaf cells overexpressing *LEC2* are PSVs. TIP3;1 was localized to the tonoplast of small leaf vacuoles from *LEC2* plants incubated on DEX (A) but not tonoplasts of large leaf LV from plants incubated on DMSO (B). In seeds, TIP3;1 was localized to the PSV tonoplast (C). LV, Lytic vacuole; OB, oil body; PSV, protein storage vacuole; V, vacuole. Arrows point to 15-nm gold particles. Bars = 100 nm (A) and 500 nm (B and C).

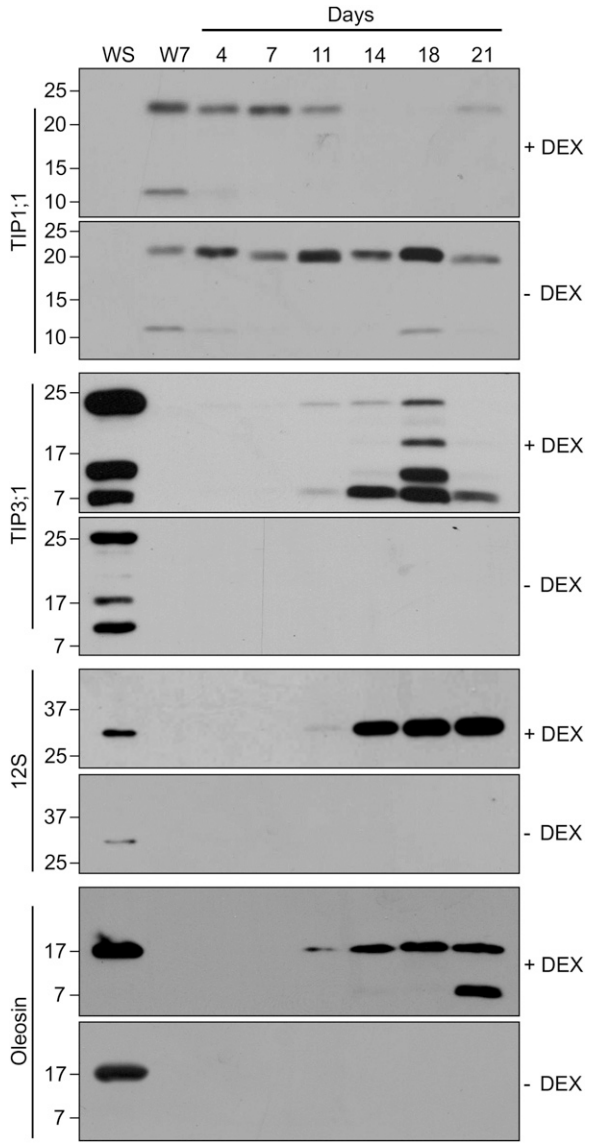

Figure 7. DEX-induced *LEC2* leaves accumulate seed proteins, while vegetative proteins disappear over time. Seedlings were treated with 30 μM DEX (+DEX) or DMSO (–DEX). Protein controls were extracted from Ws-0 seed (WS) and leaves from 14-d-old Ws-0 seedlings (collected at the 7-d time point) growing on MS medium (W7). Antibodies against seed-specific markers oleosin (approximately 18 kD), 12S globulin (approximately 30 kD), and TIP3;1 (approximately 26 kD) and an antibody against a vegetative marker, TIP1;1 (approximately 26 kD), were used to detect the presence of proteins in samples. Wells were loaded with 50 μg (TIP1;1, TIP3;1, and 12S blots) or 10 μg (oleosin blot) leaf protein and 0.5 μg (oleosin blot), 1 μg (TIP1;1 and TIP3;1 blots), or 2.5 μg (12S blot) seed protein. Top heading indicates the number of days plants were exposed to DEX.

fluorescently labeled TIP proteins was observed by fluorescence and confocal microscopy. The *TIP3-YFP/TIP1-RFP* construct was generated by Gattolin et al. (2011) to observe the PSV to LV transition during seed germination. Expression of both *TIP* isoforms is under control of their native promoters, which are developmentally and spatially regulated (Winter et al., 2007). *TIP3;1* is expressed in seed embryos and localizes to the PSV tonoplast, while *TIP1;1* is expressed in vegetative tissues and localizes to the LV tonoplast (Beebo et al., 2009; Gattolin et al., 2009, 2011). Thus, the vacuolar type present in the cell would be distinguished by a specific fluorescent protein signal (Hunter et al., 2007).

Seven-day-old *LEC2/TIP3-YFP/TIP1-RFP* seedlings were transferred to DEX and were observed over time using a stereomicroscope equipped with a filter to detect TIP3;1-YFP fluorescence. We observed the appearance of TIP3;1-YFP in leaves at approximately 14 d on DEX, and the YFP fluorescence spread throughout the leaves over time (Supplemental Fig. S4). These leaves were excised and further examined at the cellular level using confocal microscopy (Supplemental Fig. S5). Closer examination of leaves treated with DEX for 16 d shows that individual epidermal cells begin to express *TIP3;1-YFP*. Thus, a time course was carried out to follow the vacuole transition in more detail in *LEC2* leaves induced by DEX.

In *LEC2/TIP3-YFP/TIP1-RFP* embryos 2 d after stratification, *TIP3;1-YFP* was highly expressed on the PSV tonoplast of cotyledon cells, whereas *TIP1;1-RFP* expression was not detected (Fig. 8, A–C). At 6 d, the expression of TIP markers overlapped in cotyledons; TIP3;1-YFP fluorescence was becoming less intense, while TIP1;1-RFP fluorescence was strong (Fig. 8, D–F). Colocalization of both TIPs on the same tonoplast indicates a transition from PSV to LV in germinating seedlings (Gattolin et al., 2011). Seedlings were then transferred to DEX after 7 d. By 14 d (7 d on DEX), *TIP3;1-YFP* expression was undetectable in leaves and *TIP1;1-RFP* expression was observed although with lower intensity, indicating a reduction in TIP1;1-RFP (Fig. 8, G–I). The timing of the PSV to LV transition in the *LEC2* line in our study is similar to what was reported by Gattolin et al. (2011) in ecotype Columbia (Col-0) transformed with the same TIP markers. After 21 d (14 d on DEX), *TIP1;1-RFP* expression was no longer detectable in leaf epidermal cells, while *TIP3;1-YFP* expression reappeared and highlighted a different tonoplast morphology than the central LV (Fig. 8, J–L). The timing of the LV to PSV transition in leaves overexpressing *LEC2* as demonstrated by fluorescently labeled TIP isoforms (Fig. 8) was comparable to endogenous TIP protein accumulation detected by immunoblots (Fig. 7). Both reveal the expression of *TIP1;1* but not *TIP3;1* at 14 d after germination (7 d on DEX) and the subsequent reversal of their expression patterns at 21 d after germination (14 d on DEX). Taken together, these results suggest that overexpressed *TIP* isoforms follow the same temporal expression patterns as endogenous *TIP*s and demonstrates that leaf LVs transition to PSVs in response to *LEC2* overexpression.

The reappearance of *TIP3;1-YFP* expression on the tonoplast in induced *LEC2* leaf cells at 21 d after germination (14 d on DEX) was accompanied by a novel vacuole morphology that more closely resembled PSVs. Instead of the typical puzzle-shaped leaf epidermal tonoplast morphology (Fig. 8D), several smaller, TIP3-YFP-

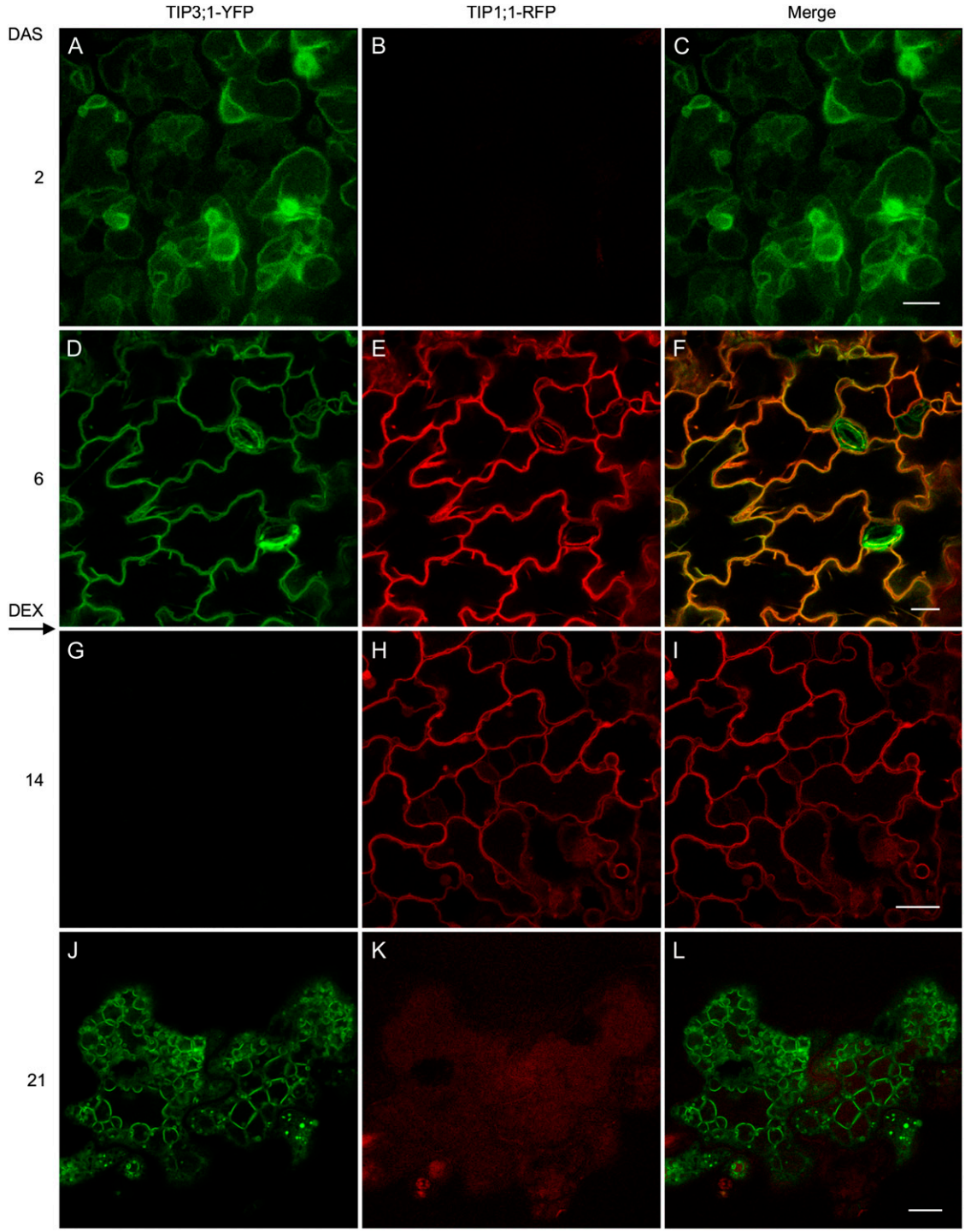

Figure 8. Leaf LVs transition to PSVs following LEC2 induction. Arabidopsis seeds coexpressing *35S:LEC2-GR*, *TIP3;1:TIP3;1-YFP* (green), and *TIP1;1:TIP1;1-RFP* (red) were germinated on MS medium for 7 d. Seedlings were then transferred to MS with 30 μM DEX (indicated by an arrow). At the indicated times, *TIP* expression was analyzed in the epidermis of cotyledons (A–F) or mature leaves (G–L) by confocal microscopy. Green oval structures in F are stomata. DAS, Days after stratification. Bars = 5 μm (A–C) and 20 μm (D–L).

labeled vacuoles appeared to occupy a large volume of the cell as shown in Figure 8J and Supplemental Figure S5D. This tonoplast configuration more closely resembles the vacuole morphology seen in embryos on day 2 (Fig. 8A). This observation shows that both *TIP* expression patterns and vacuolar morphology are substantially altered by *LEC2* overexpression.

A closer examination of plants incubated on DEX for 15 d revealed that the tonoplast labeled by TIP3;1-YFP appeared to form many fluorescent folds (Fig. 9, A

and B), like embryonic PSV tonoplasts (Fig. 9D). Additional highly fluorescent spherical structures ('bulbs') were observed (Saito et al., 2002; Beebo et al., 2009). These structures are often abundant in vacuoles of young plant tissues, and as plants mature, the number of bulbs decreases (Hunter et al., 2007). To add perspective to some images, tissues were stained with neutral red (NR), which labels the vacuole lumen (Dubrovsky et al., 2006), or with FM4-64, which, upon short incubation, labels the plasma membrane (Bolte et al., 2004). NR produced a different staining pattern in induced *LEC2* leaf vacuoles compared with embryo vacuoles. In embryos, only the globular PSV lumen was stained by NR (Fig. 9D); however, in induced *LEC2* leaves, the entire vacuolar system was stained, including the regions within folds and bulbs (Fig. 9B). To exclude the possibility that the morphological changes associated with PSV formation in induced *LEC2* leaf vacuoles was not a result of *TIP3;1-YFP* overexpression, the *TIP3;1-YFP* fusion was placed under control of a 35S constitutive promoter, thus releasing it from developmental control from its native *TIP3;1* promoter. Under the 35S promoter, *TIP3;1-YFP* is expected to localize to the tonoplast of vacuoles in every plant tissue (Hunter et al., 2007). In plants expressing *35S:TIP3;1-YFP*, leaf epidermal cell tonoplasts were fluorescently labeled by TIP3;1-YFP but had a typical puzzle-shaped LV tonoplast morphology (Fig. 9C). These results establish that the altered vacuole morphology observed in *LEC2/TIP3-YFP/TIP1-RFP* plants was caused by *LEC2* overexpression rather than simple overexpression of *TIP3;1-YFP*.

DISCUSSION

Embryonic Development Is Initiated in Leaves Overexpressing *LEC2*

LEC2 acts early during seed morphogenesis and throughout maturation to control embryo development. During morphogenesis, LEC2 acts to specify the identity of embryonic organs such as cotyledons (Harada, 2001). Mutations in *LEC2* cause the appearance of trichomes on cotyledon surfaces (Stone et al., 2001). These epidermal hairs are vegetative traits and are absent from the surface of wild-type cotyledons (Meinke, 1992; Lotan et al., 1998). We show that overexpression of *LEC2* promotes a reduced number of trichomes developing on leaves. We also show that other morphological features such as the leaf shape and texture are altered to resemble cotyledons. In addition, the leaf anatomy was modified. The organization and shape of induced *LEC2* leaf cells were similar to seed tissue. These findings are consistent with those of West et al. (1994), who demonstrated that cotyledon anatomy was altered to become more leaf like in the absence of *LEC1*, a transcription factor that shares many roles with *LEC2* (Meinke et al., 1994; To et al.,

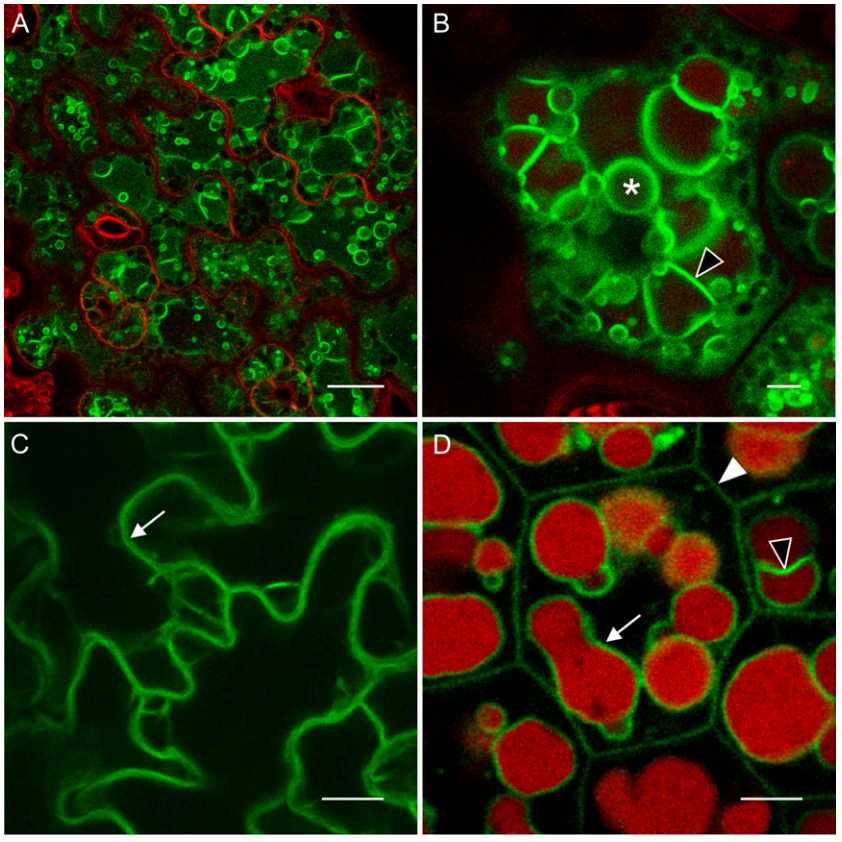

Figure 9. TIP3;1-YFP labels the tonoplast, vacuolar bulbs, and PSV-like structures that are unique to induced *LEC2* leaves and resemble embryonic storage vacuoles. A and B, *LEC2/TIP3-YFP/TIP1-RFP* plants were incubated on DEX for 15 d. Leaf epidermal cells are imaged. C, Leaves of 21-d-old plants expressing *35S:TIP3;1-YFP*. Leaf epidermal cells are imaged. D, Cotyledons of maturing *TIP3;1:TIP3;1-YFP* embryos imaged at the onset of *TIP3;1-YFP* expression. Arrows point to tonoplast, arrowhead points to plasma membrane, empty arrowheads point to tonoplast folds, and an asterisk labels a bulb. Green color is TIP3;1-YFP fluorescence. Tissues were stained red with FM4-64 to highlight the plasma membrane (A) or with NR to show the vacuole lumen (B and D). Bars = 20 μm (A) and 10 μm (B–D).

2006; Santos-Mendoza et al., 2008). Thus, the transformation in leaf morphology and anatomy upon LEC2 induction indicates that LEC2 activity causes vegetative leaves to acquire embryonic characteristics. Under our experimental conditions, the appearance of our embryo-specific markers (Supplemental Fig. S4) occurs in cells from leaves that have already differentiated. Because *LEC2* seedlings are induced very early upon germination, however, we do not know whether this fate change is programmed to occur before, during, or after the establishment of leaf primordia.

Seed storage reserves are normally accumulated in different cell types in developing seeds, depending on the species. In Arabidopsis, most reserve accumulation occurs in cotyledon cells (Mansfield and Briarty, 1992). Arabidopsis seeds typically accumulate a large amount of lipids and proteins, approximately 30% to 40% each, while starch represents only a minor storage reserve of 2% (Baud et al., 2008). Vegetative tissues generally accumulate lipids (Lin and Oliver, 2008), starch (Zeeman et al., 2007), and proteins (Staswick, 1994) only transiently, which serve as a nutrient supply when required by the plant (Baud et al., 2008). Histochemical staining of induced *LEC2* leaves showed an abnormal accumulation of lipids, starch, and protein deposits, further confirming the reprogramming of leaves toward embryogenic characteristics.

In Arabidopsis, starch is accumulated during early embryo development. However, as lipids and proteins become more abundant, starch levels fall and represent only a minor storage reserve in fully developed Arabidopsis seeds (Baud et al., 2008). Mutant *lec2* embryos were observed to increase their starch content (Meinke et al., 1994; Angeles-Núñez and Tiessen, 2012). However, overexpression of *LEC1* in *turnip* mutant hypocotyls (Casson and Lindsey, 2006) and overexpression of *LEC2* in vegetative tissues (Stone et al., 2008) also promoted an increased accumulation of starch. Similarly, we observed a 6-fold increase in starch in induced *LEC2* leaves. In these leaves, chloroplasts were filled with large starch granules and localized areas of leaf tissues had dense starch granule deposits.

LEC2 has been directly implicated in the regulation of soluble sugar and starch pathways in developing seeds (Santos-Mendoza et al., 2005; Angeles-Núñez and Tiessen, 2011, 2012). However, the means by which LEC2 regulates starch accumulation is unclear, as many of its interactions with regulators and gene targets involved in central metabolism have yet to be uncovered (Angeles-Núñez and Tiessen, 2012). Moreover, sugar signaling is an important regulatory mechanism involved in seed maturation, which is also not well understood (Gibson, 2005; Gutierrez et al., 2007). The expression of key transcriptional regulators, including *LEC2*, and several of their target genes that are involved in storage reserve synthesis are dependent on the presence of soluble sugar (Casson and Lindsey, 2006; Tsukagoshi et al., 2007).

Starch transiently accumulates in meristematic regions of vegetative tissues (Andriotis et al., 2010) and during early embryo development in Arabidopsis (da Silva et al., 1997). Embryos and meristems represent cells that are actively dividing or have recently divided and are in the early stages of differentiation. Although the importance and function of starch metabolism in these cell types is not well understood, it is thought to represent a temporary carbon reserve and is proposed to be a normal feature of cells undergoing early stages of differentiation (Andriotis et al., 2010). Similarly, the increase in leaf starch upon induction of LEC2 could be a consequence of cells altering their developmental fate to become embryonic in response to *LEC2* overexpression and therefore mimicking early embryo development. Thus, the observed increase in starch deposit and accumulation in leaves overexpressing *LEC2* further supports the idea that LEC2 promotes the change of fate of vegetative tissues toward an embryonic developmental state.

Oil bodies accumulate TAGs within a phospholipid monolayer stabilized by oleosins and other minor proteins. These organelles are typically present in TAG-accumulating organs such as seeds (Hsieh and Huang, 2004; Jolivet et al., 2004). However, in vegetative tissue ectopically expressing *LEC2*, TAG accumulation (Santos-Mendoza et al., 2005; Stone et al., 2008) and oleosin mRNA expression (Santos-Mendoza et al., 2005; Braybrook et al., 2006) was demonstrated. These findings have prompted much interest in exploiting the ability of LEC2 to activate entire seed lipid biosynthetic pathways to accumulate high levels of seed oil in leaves (Slocombe et al., 2009; Andrianov et al., 2010; Petrie et al., 2010). Our results support these previous works, and we further demonstrate the ability of LEC2 to promote oil body formation in vegetative tissues. Formation of these organelles in leaves has not previously been demonstrated.

LEC2 Causes Leaf LVs to Accumulate SSPs and Transition to PSVs

Ectopic expression of *LEC2* (Stone et al., 2008) and *FUS3* (Gazzarrini et al., 2004) was shown to promote the formation of novel protein-accumulating organelles in vegetative tissues, which were designated protein bodies but were not further characterized. In this work, we have characterized the protein-accumulating organelles to show that they resemble PSVs and accumulate SSPs. The features of the transitional vacuoles observed in leaf cells overexpressing *LEC2* closely resemble those reported in pea (*Pisum sativum*) and barley (*Hordeum vulgare*) root tip cells (Olbrich et al., 2007), in Arabidopsis tissues overexpressing *LEC1* (Junker et al., 2012), and in developing Arabidopsis (Mansfield and Briarty, 1992) and pea (Hoh et al., 1995) embryo cotyledons. However, in pea cotyledon cells, the protein deposits were contained within a tube-like membrane system that surrounded the vacuole (Hoh et al., 1995). This tubular membrane system was not observed surrounding vacuoles in

leaves overexpressing *LEC2*. Given that the coexistence of both vacuoles was observed over a very short period of time in pea (Hoh et al., 1995), a more detailed study would be required to examine the mechanism of vacuole transition in induced *LEC2* leaf cells. A recent report by Zheng and Staehelin (2011) emphasized the importance of tissue fixation on the quality of specimens by comparing PSV preservation using high-pressure freezing and freeze substitution to chemical fixation. They demonstrated that the clumped, densely stained, aggregated storage proteins in PSVs, as observed in our induced *LEC2* leaf samples, were an artifact of chemical fixation. This differs from the uniform distribution of densely stained PSV luminal contents produced by the high-pressure freezing and freeze substitution method. Earlier work by Lonsdale et al. (1999) reached the same conclusions. Ultimately, it is reasonable to consider that results by Zheng and Staehelin (2011) and Lonsdale et al. (1999), drawing attention to the differences in PSV ultrastructure between both fixation methods, together with the resemblance of our vacuole ultrastructure images to previously published works using chemical fixation (Mansfield and Briarty, 1992; Hoh et al., 1995; Olbrich et al., 2007), provide a convincing argument that the vacuolar identity is altered as a result of *LEC2* overexpression in Arabidopsis leaves.

Vegetative tissues generally have one vacuole type present in a cell at one time; however, exceptions do exist (Frigerio et al., 2008). During developmental transitions, PSVs and LVs are observed to coexist for short time periods (Hoh et al., 1995; Zheng and Staehelin, 2011). In this work, we show that while leaf cells possess LVs, upon LEC2 induction, leaf LVs transition toward PSVs that accumulate SSPs. We observed that both TIP accumulation patterns and vacuolar morphology are substantially altered by *LEC2* overexpression to become more seed-like. These PSV-like vacuoles present TIP3;1 in their tonoplast, which suggests that the vacuole has changed from a lytic to a storage function (Jauh et al., 1999). They also display tonoplast folds and bulbs, which are characteristic vacuolar configurations observed in young tissues (Saito et al., 2002). However, these vacuoles also appear to maintain a LV feature; NR staining revealed that these PSV-like vacuoles retain the large LV lumen. Thus, induced *LEC2* leaf vacuoles share similarities with both PSVs and LVs. These results also suggest that as the LV transitions toward a PSV, the tonoplast remodels before the large vacuole is replaced by smaller-sized PSVs. Because overlap of TIP1;1 and TIP3;1 proteins on the tonoplast occurs over a very short time (Fig. 7; Gattolin et al., 2011) and in induced *LEC2/TIP3-YFP/TIP1-RFP* plants, TIP1;1-RFP fluorescence is below detection (or not present) at the transitional stage to observe an overlap with TIP3;1-YFP, use of these markers cannot reveal how the vacuoles transition, only that they do transition. Therefore, a more in-depth study is needed to elucidate the LV to PSV transition and, in particular, whether this involves de novo formation of tonoplast and degradation of the preexisting LV, as observed in pea cotyledons (Hoh et al., 1995), or whether it results from a functional differentiation of the existing vacuole.

An Examination of the Transition of Leaves from a Vegetative to an Embryonic State

As *LEC2* plants are induced by DEX over time, we show that the trend is for leaves to change their developmental fate and acquire embryonic characteristics. These embryonic characteristics become obvious at 11 d on DEX. Immunoblot analysis demonstrates the accumulation of seed protein markers and the disappearance of the TIP1;1 vegetative marker from leaves over time on DEX. However, some aspects of the developmental transition caused by ectopic *LEC2* expression remain ambiguous. In triple-stained leaf sections (Supplemental Fig. S3), lipid deposits appeared as early as 4 d after exposure to DEX, whereas oleosin protein accumulation was first detected in immunoblots at 11 d after DEX treatment. The apparent discrepancy between visualization of oil bodies and oleosin accumulation could be due to a low level of accumulation of oleosin proteins earlier than 11 d that went undetected by immunoblot analysis. Santos-Mendoza et al. (2005) demonstrated that oleosin RNA transcripts were found as early as 6 h after DEX induction and levels accumulated over time. In our light microscopic images at 4 and 7 d on DEX, lipid droplets are quite small in size and few in number. However, by 11 d on DEX, when oleosin is first detected by immunoblots, oil bodies are abundant in the cytoplasm.

It is also interesting to note that at 21 d on DEX, the TIP1;1 vegetative marker reappears, while the expected 26-kD TIP3;1 protein band is absent, although its degradation product is visible. This apparent reversal of the trend toward embryogenic characteristics in leaves overexpressing *LEC2* is puzzling. *LEC2* is expressed and exerts control throughout both morphogenesis and maturation phases of seed development (Braybrook and Harada, 2008). During seed morphogenesis, LVs first form in developing embryo cells (Mansfield and Briarty, 1991; Zouhar and Rojo, 2009) and transition to PSVs as storage reserves begin accumulating in early maturation (Mansfield and Briarty, 1992). Perhaps 21 d of LEC2 activity shifts leaf cells to that early stage of maturation, where LVs are transitioning toward PSVs. The Arabidopsis eFP Browser (Winter et al., 2007) shows overlap in gene expression of both TIP isoforms at the torpedo stage of embryo development. At this stage, LVs transition to PSVs to store the accumulating seed reserves (Braybrook and Harada, 2008). However, in torpedo stage embryos, TIP1;1 is localized to vacuoles in maternal seed tissues but not in embryos (Gattolin et al., 2011). An alternate hypothesis to explain these results would be an activation of negative

seed regulators to promote plant survival, as vegetative development is dependent on LVs to maintain a rigid cell structure to support plant growth (Zouhar and Rojo, 2009). Several negative regulators have been identified that repress the seed developmental program (Tang et al., 2008, 2012a, 2012b; Zhang and Ogas, 2009; Willmann et al., 2011). Clearly, these hypotheses require more investigation.

CONCLUSION

In summary, we have shown that *LEC2* overexpression modifies the morphology and anatomy of leaves by promoting differentiation toward an embryonic pathway. At the cellular level, we have demonstrated the accumulation of storage reserves and the appearance of their respective seed storage organelles. The transition between vacuole types during vegetative to embryonic developmental phases is not well understood, thus we examined the vacuole transition in induced *LEC2* cells more closely. We showed that the large LV, typically present in leaf cells, is replaced by PSV-like organelles in response to *LEC2* overexpression. These PSV-like vacuoles bear a morphological resemblance to both embryo and leaf vacuoles. Future work will aim to further elucidate the transition between vegetative and seed vacuoles.

MATERIALS AND METHODS

Plant Material and Growth Conditions

Arabidopsis (*Arabidopsis thaliana*) ecotypes used in this study were Ws-0 and Col-0. For *LEC2* overexpression, Ws-0 plants harboring a *35S:LEC2-GR* construct were used (Stone et al., 2008). To study the localization of TIP isoforms during *LEC2* overexpression, *35S:LEC2-GR* plants were crossed to Col-0 plants carrying *TIP3;1:TIP3;1-YFP* and *TIP1;1:TIP1;1-RFP* constructs (*TIP3-YFP/TIP1-RFP*; Gattolin et al., 2011). F2 plants, hereafter referred to as *LEC2/TIP3-YFP/TIP1-RFP* were used for experiments. Plants were grown in soil at 21°C with 100 μmol m^{-2} sec^{-1} irradiance and with a 16-h-light/8-h-dark photoperiod.

Tissue Culture and Growth Conditions

Sterilized seeds were transferred to germination medium consisting of Murashige and Skoog (MS) salts (PhytoTechnology Laboratories) supplemented with full-strength MS vitamins and 0.4 mg L^{-1} thiamine-HCl, 100 mg L^{-1} myo-inositol, 30 g L^{-1} Suc, and 6.5 g L^{-1} agar, pH 5.8. Seeds were stratified for 3 to 4 d at 4°C in the dark and transferred to a growth chamber for germination. The growth chamber was set at 22°C day/18°C night with 138 μmol m^{-2} sec^{-1} irradiance and with a 16-h-light/8-h-dark photoperiod.

LEC2 Induction

To induce *LEC2* overexpression, stratified seeds were allowed to germinate and grow for 7 d on germination medium. Seedlings were then transferred to induction medium composed of MS germination medium supplemented with 30 μM DEX (Sigma-Aldrich). DEX was solubilized in DMSO. Seedlings were incubated for 14 d before leaves were collected. For each induction experiment, six to 10 seedlings were transferred to each culture dish and there were three to four dishes for each treatment. Induction experiments were repeated three times.

To observe the effects of *LEC2* overexpression over time, seedlings were transferred to induction medium and leaves were harvested at 3- to 4-d intervals over 21 d. After 14 d of incubation, plants were supplemented with a 2-mL solution of 30 μM DEX or DMSO in MS liquid to ensure a continuous exposure to the steroid. For each experiment, eight to 10 seedlings were transferred to each dish and there were five to seven dishes for each collection day. The experiment was repeated twice.

Tissue Collection

Plants were photographed with a Canon PowerShot S5 IS camera. For higher magnification images, a Nikon SMZ1500 dissecting microscope was used. Leaf tissues were harvested for protein analysis, chemical fixation for subsequent microscopy work, and starch quantification. For all experiments, leaves were harvested at the same time (6 h after the dark/light transition). Leaves were collected from *LEC2* plants displaying the strongest DEX-induced phenotype. For each treatment, leaves were sampled from all plants and were pooled.

Protein Extraction and Quantification

Leaf and seed samples were frozen in liquid nitrogen and homogenized to a fine powder using a Mixer Mill MM 300 (Retsch). For extraction of total soluble protein, the powder was suspended in cold protein extraction buffer [2% (w/v) polyvinylpolypyrrolidone, 1 mM EDTA, pH 8, 100 mM sodium L-ascorbate, 1 mM phenylmethylsulfonylfluoride, 1 μg mL^{-1} leupeptin, and 0.05% (v/v) Tween 20 in phosphate-buffered saline, pH 7]. For extraction of total protein, the powder was suspended in a buffer composed of 2% (w/v) SDS and 20 mM dithiothreitol in 50 mM Tris, pH 6.8. The solutions were clarified by centrifugation at 4°C for 10 min at 18,000*g*. The concentration of total soluble protein in extracts was measured by Bradford assay using the Bio-Rad Protein Assay kit. Total protein was quantified by the Lowry method using the Bio-Rad RC DC Protein Assay kit. Bovine serum albumin (BSA) was used as a standard for both methods.

Western-Blot Analysis

Extracted proteins were separated by 12% (w/v) SDS-PAGE gels and transferred to polyvinylidene difluoride membranes by semidry blotting. Membranes were incubated overnight at 4°C in 5% (w/v) blocking buffer (skim milk powder in Tris buffered saline-Tween 20 buffer [TBS-T, 300 mM NaCl, 0.1% (v/v) Tween 20, and 20 mM Tris, pH 7.5]) and then incubated with primary antibodies for 1 h. Primary antibodies and dilutions were rabbit-anti-12S globulin (1:50,000; Shimada et al., 2003), rabbit-anti-napin (1:500; Scarafoni et al., 2001), mouse-anti-Arabidopsis oleosin D9 (1:5,000; SemBioSys Genetics), rabbit-anti-TIP3;1 (0.2 μg mL^{-1}) and rabbit-anti-TIP1;1 (0.24 μg mL^{-1}; Jauh et al., 1998). Membranes were washed twice with TBS-T and twice with 0.5% (w/v) blocking buffer. Primary antibodies were detected for 1 h with a 1:5,000 dilution of horseradish peroxidase-conjugated goat-anti-mouse IgG (Bio-Rad) or goat-anti-rabbit IgG (Bio-Rad). All antibodies were diluted in 0.5% (w/v) blocking buffer. Bands were visualized using Amersham ECL Plus kit (GE Healthcare).

Chemical Fixation, Infiltration, and Embedding in Resin

Leaves were cut into 1-mm^2 pieces, and seeds were sliced into small pieces using a sharp razor blade. Tissues were immediately fixed in ice-cold 2.5% (v/v) glutaraldehyde and 4% (w/v) paraformaldehyde in 0.1 M sodium phosphate buffer, pH 7.4, for 2 d at 4°C with one change of fixative solution. Tissues were embedded in Spurr's resin for routine applications or LR Gold resin for immunogold labeling. To embed in Spurr's resin, tissues were either postfixed with 2% (w/v) OsO_4 for 1.5 h and incubated in 5% (w/v) uranyl acetate (UA) for 3 h or were not postfixed. Tissues were then dehydrated in a graded ethanol series, infiltrated with Spurr's resin, and polymerized at 60°C for 2 d. To embed in LR Gold resin, dehydrated tissues were infiltrated with LR Gold and polymerized at 4°C for 7 d using a Blak-Ray B-100AP UV lamp (UVP).

Light Microscopy

Specimens were cut into 2-μm-thick sections and stained with 0.05% (w/v) TBO (Sigma) in 0.1 M sodium phosphate buffer, pH 7.4, for 2 min (seed) or 10 min (leaf). For triple staining with OsO_4, TBO, and IKI, leaf sections

prepared from specimens that were postfixed with 2% (w/v) OsO_4 and 5% (w/v) UA were incubated with 0.05% (w/v) TBO for 10 min and stained with IKI (100 mM KI and 10 mM I_2) for 5 min. Coverslips were mounted with Permount (Fisher Scientific). Digital images were captured with a Zeiss Axio Imager Z1 microscope.

Transmission Electron Microscopy

Specimens were cut into 60-nm-thick sections for routine specimen analysis and for immunogold labeling experiments. For immunolabeling, specimens were blocked with goat normal serum (Aurion) for 30 min, followed by 2 h with primary antibodies diluted 1:10 with dilution buffer (0.2% [v/v] BSA-c [Aurion], 0.05% [v/v] Tween 20, and 1% [w/v] BSA in phosphate-buffered saline, pH 7.4). Specimens were then incubated for 1 h with secondary antibodies diluted 1:10 with dilution buffer. All secondary antibodies were IgG produced in goats and conjugated to either 10- or 15-nm gold particles (Aurion). Experiments were repeated at least twice for each antibody. All specimens were stained for 10 min with 5% (w/v) UA and 1 min with Reynold's lead citrate solution (2.6% lead nitrate and 3.5% sodium citrate, pH 12) and were examined with a CM-10 transmission electron microscope (Philips) operating at 80 kV.

Leaf Starch Quantification

Leaves (100 mg fresh weight) were collected and homogenized to a fine powder as described above. To determine the total starch content, samples were extracted with 80% ethanol, starch was hydrolyzed, and glucose measured following the STA-20 starch assay kit (Sigma). For each treatment, there were three dishes with four seedlings in each dish. The experiment was repeated three times.

Fluorescence and Confocal Laser Scanning Microscopy

Whole plants were examined using a Leica MZ FLIII fluorescence stereomicroscope. To observe YFP fluorescence, a standard GFP filter (excitation, BP480/40 nm; emission, LP510 nm) was used.

To observe the subcellular localization of TIP isoforms during LEC2 induction, 10 seedlings from each of 13 F2 lines coexpressing *LEC2/TIP3-YFP/TIP1-RFP* were studied. Seedlings were transferred to DEX-containing medium as described above, and plants were sampled over time. For controls, Arabidopsis plants expressing *35S:TIP3;1-YFP* (Hunter et al.. 2007) were maintained on one-half-strength MS medium for 21 d before leaves were harvested. Seeds expressing *TIP3;1:TIP3;1-YFP* (Hunter et al., 2007) were imbibed with water, and embryos were dissected from the seed coat before imaging. Imaging of embryos coexpressing *TIP3;1-YFP* and *TIP3;2-mCherry* was carried out as described previously (Gattolin et al., 2011).

For confocal microscopy, samples were directly examined or were stained before examination. To label vacuole lumens, tissues were immersed in 20 μM NR for 3 min. To label the plasma membrane, tissues were incubated in 8 nM FM4-64 (Invitrogen) for 2 min. Samples were observed using a Leica SP5 confocal laser scanning microscope. Imaging was performed using a 63× (1.4 numerical-aperture) water immersion lens. For visualization of NR, the stain was excited at 543 nm and emission was collected at 560 to 605 nm. FM4-64 was excited at 514 nm and detected at 616 to 645 nm. A 561-nm laser was used to excite RFP, and emission was detected at 553 to 638 nm. To image YFP, excitation was with a 514-nm laser and emission collected at 525 to 583 nm. Simultaneous detection of combinations of fluorophores was performed by combining the settings indicated above in the sequential scanning facility of the microscope as instructed by the manufacturer.

Supplemental Data

The following materials are available in the online version of this article.

Supplemental Figure S1. *LEC2* overexpression alters the leaf anatomy.

Supplemental Figure S2. TIP3-fluorescent protein fusions are localized to the tonoplast but can undergo degradation in the vacuolar lumen.

Supplemental Figure S3. Overexpression of *LEC2* promotes embryogenic characteristics in leaf cells, which become more pronounced over time on DEX.

Supplemental Figure S4. *TIP3;1* is synthesized de novo in leaves following LEC2 induction.

Supplemental Figure S5. *TIP3;1* is synthesized de novo in leaves following LEC2 induction.

ACKNOWLEDGMENTS

We thank John J. Harada for donating the 35S:*LEC2-GR* line and for helpful discussions, Dean Betts, Federica Brandizzi, Norman Hüner, Susanne Kohalmi, and Krzysztof Szczyglowski for their critical analysis of the work, Richard Gardiner and imaging staff at the University of Western Ontario Biotron for their advice and assistance, Angelo Kaldis, Kira Liu, Jamie McNeil, and Hong Zhu for technical support, Alex Molnar for graphical assistance, and the following scientists who provided antibodies: Ikuko Hara-Nishimura (anti-12S), Cory L. Nykiforuk (anti-oleosin), John C. Rogers (anti-TIP3;1 and TIP1;1), and Alessio Scarafoni (anti-2S).

Received May 7, 2013; accepted June 6, 2013; published June 18, 2013.

LITERATURE CITED

Andrianov V, Borisjuk N, Pogrebnyak N, Brinker A, Dixon J, Spitsin S, Flynn J, Matyszczuk P, Andryszak K, Laurelli M, et al (2010) Tobacco as a production platform for biofuel: overexpression of *Arabidopsis DGAT* and *LEC2* genes increases accumulation and shifts the composition of lipids in green biomass. Plant Biotechnol J **8:** 277–287

Andriotis VME, Pike MJ, Kular B, Rawsthorne S, Smith AM (2010) Starch turnover in developing oilseed embryos. New Phytol **187:** 791–804

Angeles-Núñez JG, Tiessen A (2011) Mutation of the transcription factor LEAFY COYLEDON2 alters the chemical composition of *Arabidopsis* seeds, decreasing oil and protein content, while maintaining high levels of starch and sucrose in mature seeds. J Plant Physiol **168:** 1891–1900

Angeles-Núñez JG, Tiessen A (2012) Regulation of *AtSUS2* and *AtSUS3* by glucose and the transcription factor LEC2 in different tissues and at different stages of Arabidopsis seed development. Plant Mol Biol **78:** 377–392

Baud S, Dubreucq B, Miquel M, Rochat C, Lepiniec L (2008) Storage reserve accumulation in Arabidopsis: metabolic and developmental control of seed filling. The Arabidopsis Book **6:** e0113 doi/10.1199/tab.0113

Bäumlein H, Miséra S, Luerssen H, Kölle K, Horstmann C, Wobus U, Müller AJ (1994) The *FUS3* gene of *Arabidopsis thaliana* is a regulator of gene expression during late embryogenesis. Plant J **6:** 379–387

Beebo A, Thomas D, Der C, Sanchez L, Leborgne-Castel N, Marty F, Schoefs B, Bouhidel K (2009) Life with and without AtTIP1;1, an Arabidopsis aquaporin preferentially localized in the apposing tonoplasts of adjacent vacuoles. Plant Mol Biol **70:** 193–209

Bolte S, Talbot C, Boutte Y, Catrice O, Read ND, Satiat-Jeunemaitre B (2004) FM-dyes as experimental probes for dissecting vesicle trafficking in living plant cells. J Microsc **214:** 159–173

Braybrook SA, Harada JJ (2008) LECs go crazy in embryo development. Trends Plant Sci **13:** 624–630

Braybrook SA, Stone SL, Park S, Bui AQ, Le BH, Fischer RL, Goldberg RB, Harada JJ (2006) Genes directly regulated by LEAFY COTYLEDON2 provide insight into the control of embryo maturation and somatic embryogenesis. Proc Natl Acad Sci USA **103:** 3468–3473

Casson SA, Lindsey K (2006) The *turnip* mutant of Arabidopsis reveals that *LEAFY COTYLEDON1* expression mediates the effects of auxin and sugars to promote embryonic cell identity. Plant Physiol **142:** 526–541

da Silva PMFR, Eastmond PJ, Hill LM, Smith AM, Rawsthorne S (1997) Starch metabolism in developing embryos of oilseed rape. Planta **203:** 480–487

Dubrovsky JG, Guttenberger M, Saralegui A, Napsucialy-Mendivil S, Voight B, Baluska F, Menzel D (2006) Neutral red as a probe for confocal laser scanning microscopy studies of plant roots. Ann Bot (Lond) **97:** 1127–1138

Frigerio L, Hinz G, Robinson DG (2008) Multiple vacuoles in plant cells: rule or exception? Traffic **9:** 1564–1570

Gattolin S, Sorieul M, Frigerio L (2010) Tonoplast intrinsic proteins and vacuolar identity. Biochem Soc Trans **38:** 769–773

Gattolin S, Sorieul M, Frigerio L (2011) Mapping of tonoplast intrinsic proteins in maturing and germinating *Arabidopsis* seeds reveals dual localization of embryonic TIPs to the tonoplast and plasma membrane. Mol Plant **4:** 180–189

Gattolin S, Sorieul M, Hunter P, Khonsari R, Frigerio L (2009) In vivo imaging of the tonoplast intrinsic protein family in Arabidopsis roots. BMC Plant Biol **9:** 133

Gazzarrini S, Tsuchiya Y, Lumba S, Okamoto M, McCourt P (2004) The transcription factor *FUSCA3* controls developmental timing in *Arabidopsis* through the hormones gibberellin and abscisic acid. Dev Cell **7:** 373–385

Gibson SI (2005) Control of plant development and gene expression by sugar signaling. Curr Opin Plant Biol **8:** 93–102

Giraudat J, Hauge BM, Valon C, Smalle J, Parcy F, Goodman HM (1992) Isolation of the Arabidopsis *ABI3* gene by positional cloning. Plant Cell **4:** 1251–1261

Gruis D, Schulze J, Jung R (2004) Storage protein accumulation in the absence of the vacuolar processing enzyme family of cysteine proteases. Plant Cell **16:** 270–290

Gutierrez L, Van Wuytswinkel O, Castelain M, Bellini C (2007) Combined networks regulating seed maturation. Trends Plant Sci **12:** 294–300

Harada JJ (2001) Role of *Arabidopsis LEAFY COTYLEDON* genes in seed development. J Plant Physiol **158:** 405–409

Hoh B, Hinz G, Jeong BK, Robinson DG (1995) Protein storage vacuoles form de novo during pea cotyledon development. J Cell Sci **108:** 299–310

Hope RG, Murphy DJ, McLauchlan J (2002) The domains required to direct core proteins of hepatitis C virus and GB virus-B to lipid droplets share common features with plant oleosin proteins. J Biol Chem **277:** 4261–4270

Hsieh K, Huang AHC (2004) Endoplasmic reticulum, oleosins, and oils in seeds and tapetum cells. Plant Physiol **136:** 3427–3434

Hunter PR, Craddock CP, Di Benedetto S, Roberts LM, Frigerio L (2007) Fluorescent reporter proteins for the tonoplast and the vacuolar lumen identify a single vacuolar compartment in Arabidopsis cells. Plant Physiol **145:** 1371–1382

Jauh G-Y, Fischer AM, Grimes HD, Ryan CA, Rogers JC (1998) δ-Tonoplast intrinsic protein defines unique plant vacuole functions. Proc Natl Acad Sci USA **95:** 12995–12999

Jauh G-Y, Phillips TE, Rogers JC (1999) Tonoplast intrinsic protein isoforms as markers for vacuolar functions. Plant Cell **11:** 1867–1882

Johanson U, Karlsson M, Johansson I, Gustavsson S, Sjövall S, Fraysse L, Weig AR, Kjellbom P (2001) The complete set of genes encoding major intrinsic proteins in Arabidopsis provides a framework for a new nomenclature for major intrinsic proteins in plants. Plant Physiol **126:** 1358–1369

Jolivet P, Roux E, d'Andrea S, Davanture M, Negroni L, Zivy M, Chardot T (2004) Protein composition of oil bodies in *Arabidopsis thaliana* ecotype WS. Plant Physiol Biochem **42:** 501–509

Junker A, Mönke G, Rutten T, Keilwagen J, Seifert M, Thi TMN, Renou J-P, Balzergue S, Viehöver P, Hähnel U, et al (2012) Elongation-related functions of LEAFY COTYLEDON1 during the development of *Arabidopsis thaliana*. Plant J **71:** 427–442

Keith K, Kraml M, Dengler NG, McCourt P (1994) *fusca3*: a heterochronic mutation affecting late embryo development in *Arabidopsis*. Plant Cell **6:** 589–600

Kim HU, Hsieh K, Ratnayake C, Huang AHC (2002) A novel group of oleosins is present inside the pollen of *Arabidopsis*. J Biol Chem **277:** 22677–22684

Kroj T, Savino G, Valon C, Giraudat J, Parcy F (2003) Regulation of storage protein gene expression in *Arabidopsis*. Development **130:** 6065–6073

Lin W, Oliver DJ (2008) Role of triacylglycerols in leaves. Plant Sci **175:** 233–237

Lonsdale JE, McDonald KL, Jones RL (1999) High pressure freezing and freeze substitution reveal new aspects of fine structure and maintain protein antigenicity in barley aleurone cells. Plant J **17:** 221–229

Lotan T, Ohto M, Yee KM, West MAL, Lo R, Kwong RW, Yamagishi K, Fischer RL, Goldberg RB, Harada JJ (1998) *Arabidopsis* LEAFY COTYLEDON1 is sufficient to induce embryo development in vegetative cells. Cell **93:** 1195–1205

Mansfield SG, Briarty LG (1991) Early embryogenesis in *Arabidopsis thaliana*. II. The developing embryo. Can J Bot **69:** 461–476

Mansfield SG, Briarty LG (1992) Cotyledon cell development in *Arabidopsis thaliana* during reserve deposition. Can J Bot **70:** 151–164

Mansfield SG, Briarty LG (1996) The dynamics of seedling and cotyledon cell development in *Arabidopsis thaliana* during reserve mobilization. Int J Plant Sci **157:** 280

Maurel C, Santoni V, Luu D-T, Wudick MM, Verdoucq L (2009) The cellular dynamics of plant aquaporin expression and functions. Curr Opin Plant Biol **12:** 690–698

Meinke DW (1992) A homoeotic mutant of *Arabidopsis thaliana* with leafy cotyledons. Science **258:** 1647–1650

Meinke DW, Franzmann LH, Nickle TC, Yeung EC (1994) *Leafy cotyledon* mutants of Arabidopsis. Plant Cell **6:** 1049–1064

Nambara E, Keith K, McCourt P, Naito S (1995) A regulatory role for the *ABI3* gene in the establishment of embryo maturation in *Arabidopsis thaliana*. Development **121:** 629–636

Olbrich A, Hillmer S, Hinz G, Oliviusson P, Robinson DG (2007) Newly formed vacuoles in root meristems of barley and pea seedlings have characteristics of both protein storage and lytic vacuoles. Plant Physiol **145:** 1383–1394

Parcy F, Valon C, Raynal M, Gaubier-Comella P, Delseny M, Giraudat J (1994) Regulation of gene expression programs during *Arabidopsis* seed development: roles of the *ABI3* locus and of endogenous abscisic acid. Plant Cell **6:** 1567–1582

Penfield S, Pinfield-Wells HM, Graham IA (2006) Storage reserve mobilisation and seedling establishment in Arabidopsis. The Arabidopsis Book**:** e0100

Petrie J, Shrestha P, Liu Q, Mansour M, Wood C, Zhou X-R, Nichols P, Green A, Singh S (2010) Rapid expression of transgenes driven by seed-specific constructs in leaf tissue: DHA production. Plant Methods **6:** 8–13

Regan SM, Moffatt BA (1990) Cytochemical analysis of pollen development in wild-type *Arabidopsis* and a male-sterile mutant. Plant Cell **2:** 877–889

Sablowski RWM, Meyerowitz EM (1998) A homolog of *NO APICAL MERISTEM* is an immediate target of the floral homeotic genes *APETALA3/PISTILLATA*. Cell **92:** 93–103

Saito C, Ueda T, Abe H, Wada Y, Kuroiwa T, Hisada A, Furuya M, Nakano A (2002) A complex and mobile structure forms a distinct subregion within the continuous vacuolar membrane in young cotyledons of Arabidopsis. Plant J **29:** 245–255

Santos-Mendoza M, Dubreucq B, Baud S, Parcy F, Caboche M, Lepiniec L (2008) Deciphering gene regulatory networks that control seed development and maturation in Arabidopsis. Plant J **54:** 608–620

Santos-Mendoza M, Dubreucq B, Miquel M, Caboche M, Lepiniec L (2005) LEAFY COTYLEDON 2 activation is sufficient to trigger the accumulation of oil and seed specific mRNAs in *Arabidopsis* leaves. FEBS Lett **579:** 4666–4670

Scarafoni A, Carzaniga R, Harris N, Croy RD (2001) Manipulation of the napin primary structure alters its packaging and deposition in transgenic tobacco (*Nicotiana tabacum* L.) seeds. Plant Mol Biol **46:** 727–739

Shaner NC, Steinbach PA, Tsien RY (2005) A guide to choosing fluorescent proteins. Nat Methods **2:** 905–909

Shimada T, Yamada K, Kataoka M, Nakaune S, Koumoto Y, Kuroyanagi M, Tabata S, Kato T, Shinozaki K, Seki M, et al (2003) Vacuolar processing enzymes are essential for proper processing of seed storage proteins in *Arabidopsis thaliana*. J Biol Chem **278:** 32292–32299

Shimada TL, Shimada T, Takahashi H, Fukao Y, Hara-Nishimura I (2008) A novel role for oleosins in freezing tolerance of oilseeds in *Arabidopsis thaliana*. Plant J **55:** 798–809

Siloto RMP, Findlay K, Lopez-Villalobos A, Yeung EC, Nykiforuk CL, Moloney MM (2006) The accumulation of oleosins determines the size of seed oilbodies in *Arabidopsis*. Plant Cell **18:** 1961–1974

Slocombe SP, Cornah J, Pinfield-Wells H, Soady K, Zhang Q, Gilday A, Dyer JM, Graham IA (2009) Oil accumulation in leaves directed by modification of fatty acid breakdown and lipid synthesis pathways. Plant Biotechnol J **7:** 694–703

Staswick PE (1994) Storage proteins of vegetative plant tissues. Annu Rev Plant Physiol Plant Mol Biol **45:** 302–322

Stone SL, Braybrook SA, Paula SL, Kwong LW, Meuser J, Pelletier J, Hsieh T-F, Fischer RL, Goldberg RB, Harada JJ (2008) *Arabidopsis* LEAFY COTYLEDON2 induces maturation traits and auxin activity: implications for somatic embryogenesis. Proc Natl Acad Sci USA **105:** 3151–3156

Stone SL, Kwong LW, Yee KM, Pelletier J, Lepiniec L, Fischer RL, Goldberg RB, Harada JJ (2001) *LEAFY COTYLEDON2* encodes a B3 domain transcription factor that induces embryo development. Proc Natl Acad Sci USA **98:** 11806–11811

Tamura K, Shimada T, Ono E, Tanaka Y, Nagatani A, Higashi S, Watanabe M, Nishimura M, Hara-Nishimura I (2003) Why green

fluorescent fusion proteins have not been observed in the vacuoles of higher plants. Plant J **35:** 545–555

Tang X, Bian S, Tang M, Lu Q, Li S, Liu X, Tian G, Nguyen V, Tsang EWT, Wang A, et al (2012a) MicroRNA–mediated repression of the seed maturation program during vegetative development in *Arabidopsis*. PLoS Genet **8:** e1003091

Tang X, Hou A, Babu M, Nguyen V, Hurtado L, Lu Q, Reyes JC, Wang A, Keller WA, Harada JJ, et al (2008) The Arabidopsis BRAHMA chromatin-remodeling ATPase is involved in repression of seed maturation genes in leaves. Plant Physiol **147:** 1143–1157

Tang X, Lim M-H, Pelletier J, Tang M, Nguyen V, Keller WA, Tsang EWT, Wang A, Rothstein SJ, Harada JJ, et al (2012b) Synergistic repression of the embryonic programme by SET DOMAIN GROUP 8 and EMBRYONIC FLOWER 2 in *Arabidopsis* seedlings. J Exp Bot **63:** 1391–1404

To A, Valon C, Savino G, Guilleminot J, Devic M, Giraudat J, Parcy F (2006) A network of local and redundant gene regulation governs *Arabidopsis* seed maturation. Plant Cell **18:** 1642–1651

Tsukagoshi H, Morikami A, Nakamura K (2007) Two B3 domain transcriptional repressors prevent sugar-inducible expression of seed maturation genes in *Arabidopsis* seedlings. Proc Natl Acad Sci USA **104:** 2543–2547

Vicente-Carbajosa J, Carbonero P (2005) Seed maturation: developing an intrusive phase to accomplish a quiescent state. Int J Dev Biol **49:** 645–651

West MAL, Yee KM, Danao J, Zimmerman JL, Fischer RL, Goldberg RB, Harada JJ (1994) *LEAFY COTYLEDON1* is an essential regulator of late embryogenesis and cotyledon identity in *Arabidopsis*. Plant Cell **6:** 1731–1745

Willmann MR, Mehalick AJ, Packer RL, Jenik PD (2011) MicroRNAs regulate the timing of embryo maturation in Arabidopsis. Plant Physiol **155:** 1871–1884

Winter D, Vinegar B, Nahal H, Ammar R, Wilson GV, Provart NJ (2007) An "electronic fluorescent pictograph" browser for exploring and analyzing large-scale biological data sets. PLoS ONE **2:** e718

Zeeman SC, Smith SM, Smith AM (2007) The diurnal metabolism of leaf starch. Biochem J **401:** 13–28

Zhang H, Ogas J (2009) An epigenetic perspective on developmental regulation of seed genes. Mol Plant **2:** 610–627

Zheng H, Staehelin LA (2011) Protein storage vacuoles are transformed into lytic vacuoles in root meristematic cells of germinating seedlings by multiple, cell type-specific mechanisms. Plant Physiol **155:** 2023–2035

Zouhar J, Rojo E (2009) Plant vacuoles: where did they come from and where are they heading? Curr Opin Plant Biol **12:** 677–684